

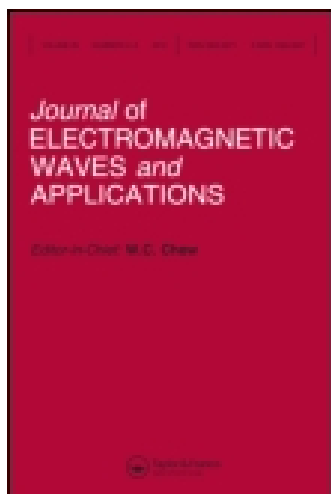
This article was downloaded by: [University of New Mexico]

On: 14 October 2014, At: 16:21

Publisher: Taylor & Francis

Informa Ltd Registered in England and Wales Registered Number: 1072954

Registered office: Mortimer House, 37-41 Mortimer Street, London W1T 3JH, UK



## Journal of Electromagnetic Waves and Applications

Publication details, including instructions for authors and subscription information:

<http://www.tandfonline.com/loi/tewa20>

### A Miniaturized Dual-band Power Divider with Harmonic Suppression for Gsm Applications

W. Huang<sup>a</sup>, C. Liu<sup>b</sup>, L. Yan<sup>c</sup> & K. Huang<sup>d</sup>

<sup>a</sup> School of Electronics and Information Engineering, Sichuan University, Chengdu 610064, China

<sup>b</sup> School of Electronics and Information Engineering, Sichuan University, Chengdu 610064, China

<sup>c</sup> School of Electronics and Information Engineering, Sichuan University, Chengdu 610064, China

<sup>d</sup> School of Electronics and Information Engineering, Sichuan University, Chengdu 610064, China

Published online: 03 Apr 2012.

To cite this article: W. Huang, C. Liu, L. Yan & K. Huang (2010) A Miniaturized Dual-band Power Divider with Harmonic Suppression for Gsm Applications, Journal of Electromagnetic Waves and Applications, 24:1, 81-91, DOI: [10.1163/156939310790322082](https://doi.org/10.1163/156939310790322082)

To link to this article: <http://dx.doi.org/10.1163/156939310790322082>

PLEASE SCROLL DOWN FOR ARTICLE

Taylor & Francis makes every effort to ensure the accuracy of all the information (the "Content") contained in the publications on our platform. However, Taylor & Francis, our agents, and our licensors make no representations or warranties whatsoever as to the accuracy, completeness, or suitability for any purpose of the Content. Any opinions and views expressed in this publication are the opinions and views of the authors, and are not the views of or endorsed by Taylor & Francis. The accuracy of the Content should not be relied upon and should be independently verified with primary sources of information. Taylor and Francis shall not be liable for any losses, actions, claims, proceedings, demands, costs, expenses, damages, and other liabilities whatsoever or howsoever caused

arising directly or indirectly in connection with, in relation to or arising out of the use of the Content.

This article may be used for research, teaching, and private study purposes. Any substantial or systematic reproduction, redistribution, reselling, loan, sub-licensing, systematic supply, or distribution in any form to anyone is expressly forbidden. Terms & Conditions of access and use can be found at <http://www.tandfonline.com/page/terms-and-conditions>

## A MINIATURIZED DUAL-BAND POWER DIVIDER WITH HARMONIC SUPPRESSION FOR GSM APPLICATIONS

W. Huang, C. Liu, L. Yan, and K. Huang

School of Electronics and Information Engineering  
Sichuan University  
Chengdu 610064, China

**Abstract**—In this paper, a miniaturized dual-band power divider based on artificial transmission lines is proposed for GSM applications. The design consists of four sections of recently developed planar artificial transmission lines, an LC tank circuit in shunt, and an isolation resistor. The experimental results show that the proposed configuration has good performance at both 0.9 GHz and 1.8 GHz. Meanwhile, it achieves a significant size reduction compared to traditional dual-band planar power dividers. At the center frequency 1.35 GHz, the dimension of the proposed dual-band power divider is only  $43\text{ mm} \times 21\text{ mm}$ , or equivalently  $0.29\lambda_g \times 0.14\lambda_g$ . With the harmonic suppression nature of artificial transmission lines and the shunt LC tank, the wideband response of the proposed dual-band power divider reveals good harmonics suppression.

### 1. INTRODUCTION

Power dividers, as a basic component, are widely applied to microwave and millimeter-wave systems including antenna arrays, power amplifiers, mixers, etc. [1–4]. In order to make better use of spectrum resources and improve the signal transmission efficiency, dual-band and multi-frequency communication circuits have become increasingly popular for various applications. However, a traditional Wilkinson power divider usually works at the specified frequency and its odd harmonics [5]. A power divider designed for two or more frequency bands can not only effectively reduce the circuit size but also lower the insertion loss. In recent years, various techniques

---

Corresponding author: C. Liu (cjliu@ieee.org).

to implement dual-band power dividers have been proposed. Dual-band power dividers using two sections of transformers [6, 7], open or short stub lines [8–11], or adding extra lumped inductor and lumped capacitor in parallel with isolation resistor [12, 13], have been proposed.

This paper presents a novel miniaturized dual-band power divider with recently proposed planar artificial transmission lines. An LC tank circuit is applied to further reducing its size. The new design is composed of four sections of quarter-wavelength artificial transmission lines, which are used to take place of traditional microstrip transmission lines. Simulated and measured results agree well with each other. It is found that the power divider shows excellent performances : a) size reduction, only  $0.29\lambda_g \times 0.14\lambda_g$ ; b) low insertion loss, less than 3.6 dB; and c) good harmonics suppression.

## 2. ANALYSIS AND DESIGN OF PLANAR ARTIFICIAL TRANSMISSION LINE

Recently, Wang proposed the concept of artificial transmission lines [14], which is composed of three cascade stages of quasi-lumped inductors and capacitors. The layout and equivalent circuit of a section of artificial transmission line are shown in Fig. 1, respectively. The design concept and methodology have been presented in details in [14]. Artificial transmission lines instead of conventional microstrip transmission lines can reduce physical dimensions of microwave components greatly, especially at low frequency band.

Referring to the equivalent lumped circuit in Fig. 1(b), the inductors  $L_1$ ,  $L_2$  and  $L_3$  represent meandered-line inductors. The parasitic capacitance of  $L_1$  and  $L_3$  are represented by capacitors  $C_{l1}$ ,  $C_{l2}$  and  $C_{l3}$ ,  $C_{l4}$ , respectively. The series capacitance  $C_1$  and  $C_2$  are realized by two interdigital capacitors.  $C_{p1}$ ,  $C_{p2}$ ,  $C_{p3}$ ,  $C_{p4}$  are parasitic capacitance of meandered-line inductor  $L_2$  and interdigital capacitors  $C_1$  and  $C_2$ . The shunt capacitors  $C_{s1}$ ,  $C_{s2}$ ,  $C_{s3}$ ,  $C_{s4}$  are implemented with microstrip parallel-plate capacitors, which are shunt to the parasitic capacitors  $C_{p1}$ ,  $C_{p2}$ ,  $C_{p3}$ ,  $C_{p4}$ . The characteristic impedance  $Z_{ATL}$  and guided wavenumber  $\beta_{g,ATL}$  of the artificial transmission line are given by

$$Z_{ATL} = \sqrt{L_{tot}/C_{tot}} \quad (1)$$

$$\beta_{g,ATL} = \omega \sqrt{L_{tot} \cdot C_{tot}} \quad (2)$$

where  $L_{tot} = L_1 + L_2 + L_3$ ,  $C_{tot} = C_{l1} + C_{l2} + C_{l3} + C_{l4} + C_{p1} + C_{p2} + C_{p3} + C_{p4} + C_{s1} + C_{s2} + C_{s3} + C_{s4}$ , and  $\omega$  is the angle frequency.

If  $L_{tot}$  and  $C_{tot}$  increase proportionally, the guided wavenumber increases as well while the characteristic impedance remains

unchanged. Thus, the required physical length of a microstrip line is reduced significantly by decreasing the guided wavelength  $\lambda_g$ .

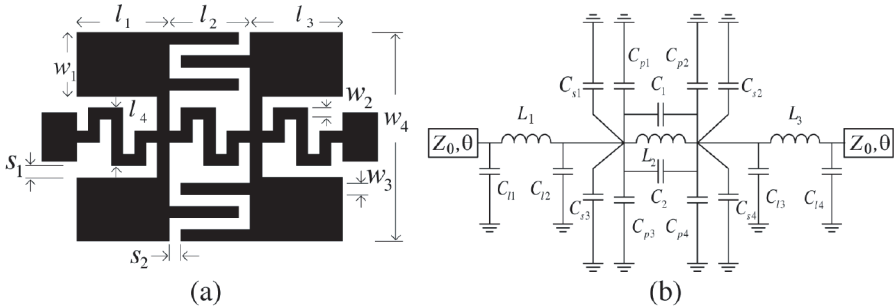


**Figure 1.** A section of artificial transmission line and its equivalent circuit.

**Table 1.** Element values of the artificial transmission section of  $57.7 \Omega$  characteristic impedance and electric length of  $90^\circ$ .

Element	Value	Element	Value	Element	Value
$C_{l1}$	0.10 pF	$C_{p1}$	0.18 pF	$C_{s3}$	0.32 pF
$C_{l2}$	0.10 pF	$C_{p2}$	0.09 pF	$C_{s4}$	0.32 pF
$C_{l3}$	0.10 pF	$C_{p3}$	0.09 pF	$L_1$	2.59 nH
$C_{l4}$	0.10 pF	$C_{p4}$	0.18 pF	$L_2$	2.59 nH
$C_1$	0.08 pF	$C_{s1}$	0.32 pF	$L_3$	2.59 nH
$C_2$	0.08 pF	$C_{s2}$	0.32 pF	$\theta$	28.47 Degree

According to the above mentioned criteria, an artificial transmission line with a characteristic impedance of  $57.7 \Omega$  and an electrical length of  $90^\circ$  was designed on a 1 mm substrate F4B-2 with dielectric constant of 2.65 and loss tangent of 0.001. The element values of the artificial transmission line are summarized in Table 1. However, the dimensions of the line still need fine tuning by full-wave simulation software (Zeland IE3D) to take parasitic couplings between those elements into consideration. The optimized parameters are given by  $l_1 = l_3 = 3.4$  mm,  $l_2 = 2.8$  mm,  $l_4 = 2.4$  mm,  $w_1 = 2.2$  mm,  $w_2 = w_3 = 0.4$  mm,  $w_4 = 7.6$  mm and  $s_1 = 0.4$  mm,  $s_2 = 0.2$  mm. The center frequency is 1.35 GHz, which is the center frequency of a dual-frequency, i.e., 900 MHz and 1800 MHz, GSM system.

Two extra conventional microstrip lines are appended to both ends of the artificial transmission line with phase shift  $28.47^\circ$  to complete the transmission line. The simulated impedance of the transmission line is  $57.7 \Omega$ , and the phase shift at 1.35 GHz is  $89.8^\circ$ . The physical length of the artificial transmission line is less than 60% of the guided wavelength at 1.35 GHz.

### 3. PROTOTYPE OF DUAL-BAND POWER DIVIDER

The dual-band power divider is basically composed of four branch lines of quarter wavelength ( $Z_A$  and  $Z_B$ ), an open circuit stub of quarter wavelength in shunt ( $Z_C$ ), and an isolation resistor  $R$  [9], as shown in Fig. 2. It is designed to work at dual frequencies  $f_1$  and  $f_2$ .

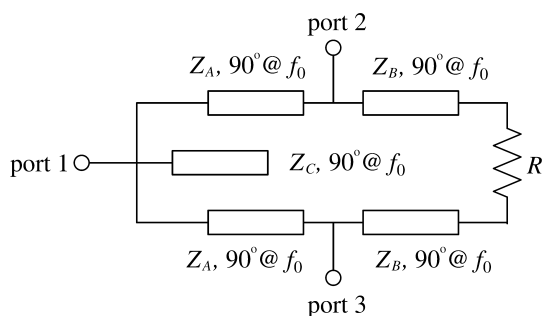


**Figure 2.** Dual-band power divider topology.

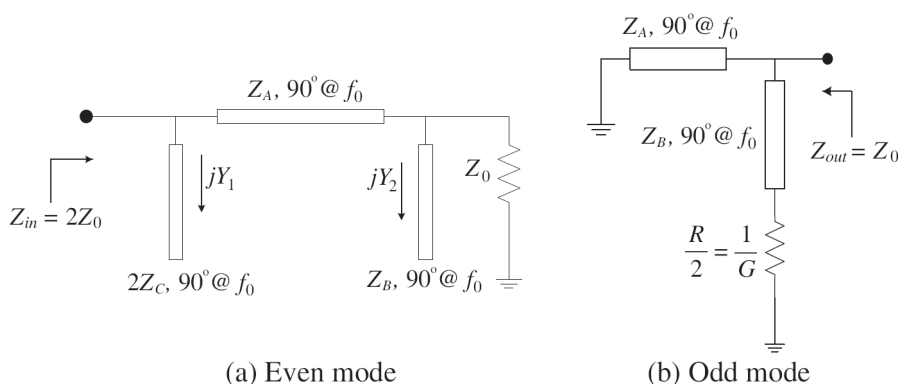


**Figure 3.** Half circuit of the dual-band power divider at even and odd modes.

### 3.1. Even-mode Analysis

It is noticed that the even-mode circuit is composed of a series line and two shunt branches in Fig. 3(a). The ABCD matrix can be expressed as

$$\begin{bmatrix} A & B \\ C & D \end{bmatrix} = \begin{bmatrix} 1 & 0 \\ jY_1 & 1 \end{bmatrix} \begin{bmatrix} \cos \theta & jZ_A \sin \theta \\ jY_A \sin \theta & \cos \theta \end{bmatrix} \begin{bmatrix} 1 & 0 \\ jY_2 & 1 \end{bmatrix} \quad (3)$$

where  $\theta = \frac{\pi}{2} \cdot \frac{f}{f_0}$ ,  $Y_A = \frac{1}{Z_A}$ ,  $Y_B = \frac{1}{Z_B}$ ,  $Y_C = \frac{1}{Z_C}$ ,  $Y_1 = \frac{1}{2}Y_C \tan \theta$ ,  $Y_2 = Y_B \tan \theta$ , and  $f_0 = \frac{f_1+f_2}{2}$ . The above matrix can be expanded to give

$$A = \cos \theta - Y_2 Z_A \sin \theta \quad (4)$$

$$B = jZ_A \sin \theta \quad (5)$$

$$D = \cos \theta - Y_1 Z_A \sin \theta \quad (6)$$

When the output port is matched, we obtain

$$\begin{bmatrix} A & B \\ C & D \end{bmatrix} \begin{bmatrix} 1 & 0 \\ \frac{1}{Z_0} & 1 \end{bmatrix} = \begin{bmatrix} A + \frac{B}{Z_0} & B \\ C + \frac{D}{Z_0} & D \end{bmatrix} \quad (7)$$

Consequently, the input impedance is

$$Z_{in} = \frac{AZ_0 + B}{CZ_0 + D} = 2Z_0 \quad (8)$$

Then, we obtain

$$Z_C = \frac{Z_A}{k_E + \cot^2 \theta} \quad (9)$$

$$Z_A^2 Y_0^2 = 2 + \cot^2 \theta + 2k_E - k_E^2 \tan^2 \theta \quad (10)$$

where  $k_E = \frac{Z_A}{Z_B}$  and  $Y_0 = \frac{1}{Z_0}$ .

### 3.2. Odd-mode Analysis

The output admittance is given by

$$Y_{out} = Y_0 = Y_B \frac{G + jY_B \tan \theta}{Y_B + jG \tan \theta} - jY_A \cot \theta \quad (11)$$

The above equation equals to

$$G = \frac{Y_0}{1 + \frac{1}{k_O}} \quad (12)$$

$$\frac{Z_A^2 Y_0^2}{1 + k_O} = k_O - \cot^2 \theta \quad (13)$$

where  $k_O = \frac{1+\sqrt{1+8\tan^2\theta}}{2\tan^2\theta}$ .

We find that the equations have the same solution at both the upper and the lower band frequencies  $f_1$  and  $f_2$ . It shows that  $k_O = k_E = k$  as well. By using the odd-mode and even-mode analysis, the circuit parameters can be determined by

$$Z_A = Z_0 \sqrt{(1+k)(k - \tan^2 \varepsilon)} \quad (14)$$

$$Z_B = \frac{Z_A}{k} \quad (15)$$

$$Z_C = \frac{Z_A}{k + \tan^2 \varepsilon} \quad (16)$$

$$R = 2Z_0 (1 + k^{-1}) \quad (17)$$

where  $k = \frac{1+\sqrt{1+8\cot^2\varepsilon}}{2\cot^2\varepsilon}$ , and  $\varepsilon = \frac{\pi}{2} \cdot \frac{f_2/f_1 - 1}{f_2/f_1 + 1}$ .

From the previously derived equations, an arbitrary dual-band power divider is achieved with this circuit topology.

We want to design a power divider at two frequencies of  $f_1 = 0.9$  GHz and  $f_2 = 1.8$  GHz. From the previously derived Formulas (14)–(17) the values of  $Z_A$  and  $Z_B$ ,  $Z_C$  and  $R$  are calculated to be  $57.7 \Omega$ ,  $57.7 \Omega$ ,  $43.3 \Omega$  and  $200 \Omega$ , respectively.

#### 4. SHORT-CIRCUITED LC TANK ANALYSIS

It is showed in Fig. 4 that a short-circuited LC tank circuit is employed instead of the open circuit transmission line of quarter wavelength in shunt, and consequently the dimension of the dual-band power divider is reduced further. It is proved that Fig. 2 and Fig. 4 have the same characteristics in the vicinity of  $\omega = \omega_0$ .

The impedance of the LC tank circuit in Fig. 4 is written as

$$Z_{LC} = j\omega L + \frac{1}{j\omega C} = j\sqrt{\frac{L}{C}} \left( \frac{\omega}{\omega_0} - \frac{\omega_0}{\omega} \right) \quad (18)$$

And the impedance of open circuit line of quarter wavelength is

$$Z_{open} = \frac{-jZ_0}{\tan(\beta l)} = \frac{-jZ_0}{\tan\left(\frac{\pi}{2} \cdot \frac{\omega}{\omega_0}\right)} \quad (19)$$

We use Taylor series to expand the above two equations at  $\omega_0$ , respectively, and make the first order approximation. Hence, the

solutions are

$$Z_C = \frac{4}{\pi} \sqrt{\frac{L}{C}} \quad (20)$$

$$f_0 = \frac{1}{2\pi\sqrt{LC}} \quad (21)$$

From above equations the values of  $L$  and  $C$  are calculated to be 4 nH and 3.5 pF, respectively, and the LC tank circuit is shorted to ground. The final  $L$  and  $C$  values, however, still need further tuning to account for the parasitic effects of chip elements and the via hole to ground. Therefore, the optimized values of  $L$  and  $C$  are 3.3 nH and 3.3 pF, respectively, based on full-wave simulations.

Figure 5 compares the wideband response of the dual-band power divider with short-circuited LC tank and with open quarter wavelength in shunt, from 0.5 GHz to 10 GHz. For the power divider with LC tank in shunt, the simulated attenuation at the output ports is better than 15 dB from 4.3 GHz to 10 GHz. At harmonic frequencies, the LC tank design shows a better frequency response compared with the open circuit line design. Therefore, the dual-band power divider has good harmonic suppression.

## 5. SIMULATIONS AND MEASUREMENTS

A miniaturized dual-band power divider is designed and realized by implementing artificial transmission lines. It was fabricated on a 1 mm

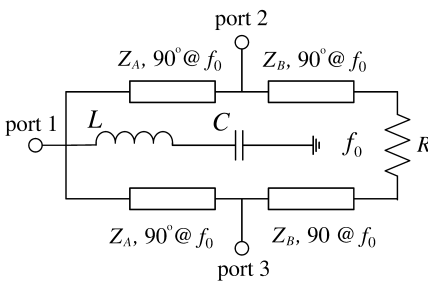


**Figure 4.** Dual-band power divider topology with LC tank.

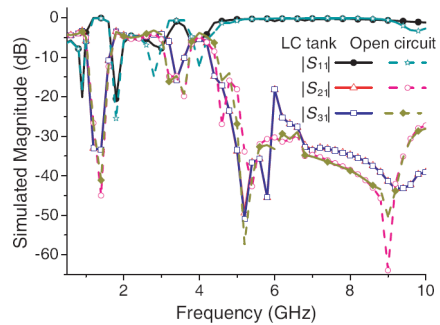


**Figure 5.** Comparison of the  $S$  parameters for the dual-band power dividers using short-circuited LC tank and open circuit transmission line.

F4B-2 substrate with dielectric constant of 2.65 and loss tangent of 0.0001, and two frequencies are  $f_1 = 0.9$  GHz and  $f_2 = 1.8$  GHz with a frequency ratio of 2 for GSM applications. Following the design procedures previously discussed in Sections 2 to 4, the characteristic impedances and electrical lengths of the transmission lines for the power divider are

$$\begin{cases} Z_A = 57.7 \Omega, \theta_A = 90^\circ @ 1.35 \text{ GHz} \\ Z_B = 57.7 \Omega, \theta_B = 90^\circ @ 1.35 \text{ GHz} \\ L = 3.3 \text{ nH}, C = 3.3 \text{ pF}, R = 200 \Omega \end{cases} \quad (22)$$

where  $Z_A$ ,  $Z_B$ ,  $L$ ,  $C$ , and  $R$  are as shown in Fig. 4.

The complete layout of fabricated power divider is shown in Fig. 6. Its size is  $43 \text{ mm} \times 21 \text{ mm}$ , or equivalently  $0.29\lambda_g \times 0.14\lambda_g$ . Here  $\lambda_g$  denotes the guided wavelength of conventional  $57.7 \Omega$  microstrip line at 1.35 GHz. Compared with the conventional microstrip dual-band power divider as used in the prototype, our design features a size reduction as high as 58%. The simulation and measurement results (from an Agilent N5230A vector network analyzer) of this

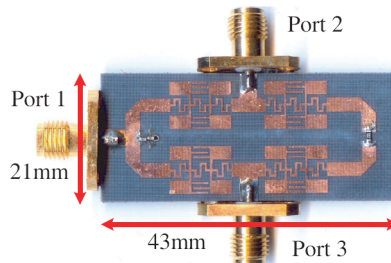


**Figure 6.** Photo of the fabricated dual-band power divider.

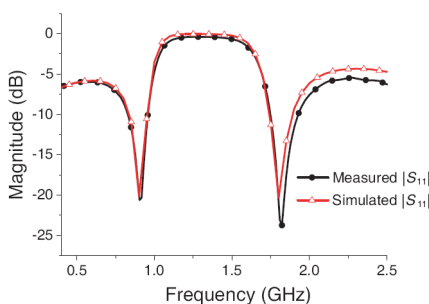


**Figure 7.** Simulated and measured  $|S_{11}|$ .

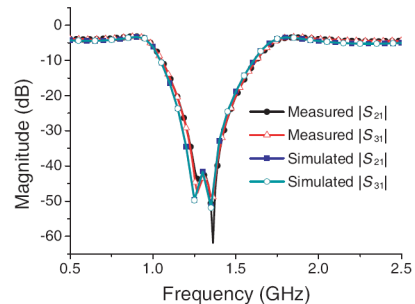


**Figure 8.** Simulated and measured  $|S_{21}|$  and  $|S_{31}|$ .

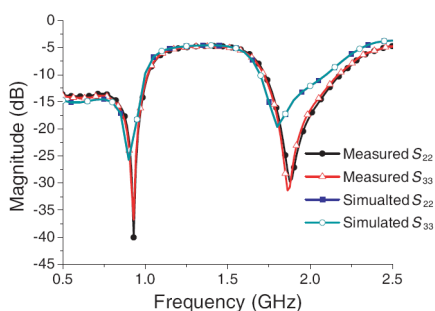


**Figure 9.** Simulated and measured  $|S_{22}|$  and  $|S_{33}|$ .

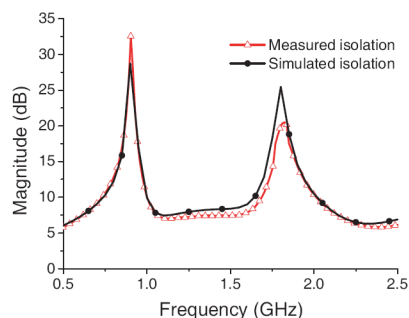
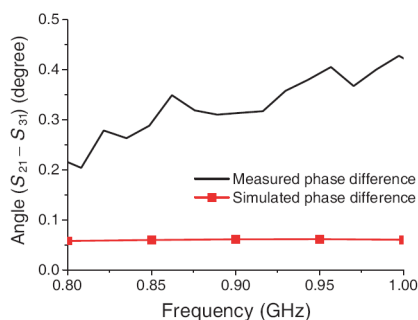
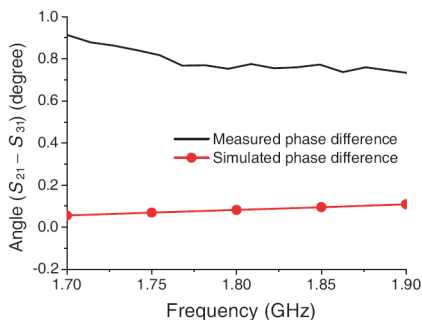


**Figure 10.** Simulated and measured isolations.



(a) The lower band



(b) The upper band

**Figure 11.** Simulated and measured phase difference.

power divider are plotted from Fig. 7 to Fig. 11. There is a good agreement between simulations and measurements. The measured center frequencies of two operational bands are 0.9 GHz and 1.81 GHz, respectively, which are very close to the design. The measured  $|S_{11}|$  as shown in Fig. 7 is below  $-20$  dB at 0.9 GHz and 1.81 GHz. As shown in Fig. 8, the transmissions to output ports are  $|S_{21}| = -3.22$  dB and  $|S_{31}| = -3.28$  dB at 0.9 GHz, and  $|S_{21}| = -3.51$  dB and  $|S_{31}| = -3.45$  dB at 1.81 GHz, respectively. Fig. 9 plots the reflection coefficients of output ports  $|S_{22}|$  and  $|S_{33}|$ , showing that both are below  $-30$  dB at the two operational frequencies. Fig. 10 plots the isolation between two output ports, showing that both are higher than 20 dB at two operating frequencies. Fig. 11 gives the phase response, showing the phase difference between port 2 and port 3 ( $Angle(S_{31}) - Angle(S_{21})$ ) are  $0.31^\circ$  at 0.9 GHz and  $0.77^\circ$  at 1.81 GHz. In summary, the simulations and measurements are in good agreement.

Furthermore, the bandwidth of the dual-band power divider is under the condition of equal magnitude with 0.1 dB mismatch, equal phase responses with  $1^\circ$  mismatch and good isolation (higher than 20 dB). The operating bandwidths are 140 MHz and 190 MHz at the lower band and the upper band, respectively.

## 6. CONCLUSION

In this paper, a novel miniaturized dual-band power divider has been demonstrated at 0.9 GHz and 1.8 GHz. With the even- and odd-mode analysis, the explicit design equations for dual-band power divider are presented. This novel dual-band power divider is realized by artificial transmission lines and short-circuited LC tank. It features low insertion losses, negligible magnitude and phase imbalance, and a size reduction as high as 58%. In addition, by introducing artificial transmission lines and short-circuited LC tank, the dual-band power divider exhibits good harmonic suppression. The simulations are in good agreement with experimental results. The measured results showed that the dual-band power divider works well at both assigned operational frequencies.

## ACKNOWLEDGMENT

This work was supported in part by the National Science Foundation of China under Grant 60971051 and the Youth Foundation of Sichuan Province.

## REFERENCES

1. Chen, H. and Y. Zhang, "A novel compact planar six-way power divider using folded and hybrid-expanded coupled lines," *Progress In Electromagnetics Research*, PIER 76, 243–252, 2007.
2. Oraizi, H. and M. S. Esfahlan, "Miniaturization of Wilkinson power dividers by using defected ground structures," *Progress In Electromagnetics Research Letters*, Vol. 4, 113–120, 2008.
3. Fan, F., Z.-H. Yan, and J.-B. Jiang, "Design of a novel compact power divider with harmonic suppression," *Progress In Electromagnetics Research Letters*, Vol. 5, 151–157, 2008.
4. Shamsinejad, S., M. Soleimani, and N. Komjani, "Novel miniaturized Wilkinson power divider for 3G mobile receivers," *Progress In Electromagnetics Research Letters*, Vol. 3, 9–16, 2008.

5. Wilkinson, E., "An N-way hybrid power divider," *IRE Transaction on Microwave Theory and Techniques*, Vol. 8, No. 1, 116–118, January 1960.
6. Srisathit, S., M. Chongcheawchamnan, and A. Worapishet, "Design and realization of dual-band 3 dB power divider based on two-section transmission-line topology," *Electronics Letters*, Vol. 39, No. 9, 723–724, May 2003.
7. Wu, L., Z. Sun, H. Yilmaz, and M. Berroth, "A dual-frequency Wilkinson power divider," *IEEE Transactions on Microwave Theory and Technique*, Vol. 54, No. 1, 278–284, January 2006.
8. Cheng, K.-K. M. and F.-L. Wong, "A new Wilkinson power divider design for dual-band application," *IEEE Microwave and Wireless Components Letters*, Vol. 17, No. 9, 664–666, September 2007.
9. Cheng, K.-K. M. and C. Law, "A novel approach to the design and implementation of dual-band power divider," *IEEE Transaction on Microwave Theory and Techniques*, Vol. 56, No. 2, 487–492, February 2008.
10. Park, M.-J. and B. Lee, "A dual-band Wilkinson power divider," *IEEE Microwave and Wireless Component Letters*, Vol. 18, No. 2, 85–87, February 2008.
11. Wu, Y., Y. Liu, and Y. Zhang, "A dual-band unequal Wilkinson power divider without reactive components," *IEEE Transactions on Microwave Theory and Techniques*, Vol. 57, No. 1, 216–222, January 2009.
12. Yang, T., C. Liu, L. Yan, and K. Huang, "A compact dual-band power divider using planar artificial transmission lines for GSM/DCS applications," *Progress In Electromagnetics Research Letters*, Vol. 10, 185–191, 2009.
13. Wu, L., H. Yilmaz, T. Bitzer, A. Pascht, and M. Berroth, "A dual-frequency Wilkinson power divider: For a frequency and its first harmonic," *IEEE Microwave and Wireless Components Letters*, Vol. 15, No. 2, 107–109, February 2005.
14. Wang, C.-W., T.-G. Ma, and C.-F. Yang, "A new planar artificial transmission line and its applications to a miniaturized butler matrix," *IEEE Transactions on Microwave Theory and Techniques*, Vol. 55, No. 12, December 2007.